Why is terrestrial subduction one-sided?

Taras V. Gerya ⎤ Department of Earth Sciences, Swiss Federal Institute of Technology (ETH - Zürich),
James A.D. Connolly ⎦ CH-8092 Zürich, Switzerland
David A. Yuen University of Minnesota Supercomputing Institute and Department of Geology and Geophysics,
⠀⠀⠀⠀⠀⠀⠀⠀⠀⠀⠀University of Minnesota, Minneapolis, Minnesota 55455-0219, USA

ABSTRACT

Subduction of the lithosphere at convergent-plate boundaries takes place asymmetrically—the subducted slab sinks downward, while the overriding plate moves horizontally (one-sided subduction). In contrast, global mantle convection models generally predict downwelling of both plates at convergent margins (two-sided subduction). We carried out two-dimensional (2-D) numerical experiments with a mineralogical-thermomechanical viscoelastic-plastic model to elucidate the cause of one-sided subduction. Our experiments show that the stability, intensity, and mode of subduction depend mainly on slab strength and the amount of weak hydrated rocks present above the slab. Two-sided subduction occurs at low slab strength ($\sin[\varphi] < 0.15$, where φ is effective internal friction angle), regardless of the extent of hydration. In contrast, steady-state one-sided subduction requires a weak hydrated slab interface and high slab strength ($\sin[\varphi] > 0.15$). The weak interface is maintained by the release of fluids from the subducted oceanic crust as a consequence of metamorphism. The resulting weak interplate zone localizes deformation at the interface and decouples the strong plates, facilitating asymmetric plate movement. Our work suggests that high plate strength and the presence of water are major factors controlling the style of plate tectonics driven by self-sustaining one-sided subduction processes.

Keywords: subduction zones, water, numerical modeling, slab dehydration, fluid flow.

INTRODUCTION

Seismic tomography has revealed the structure of subduction zones in a variety of geodynamic settings (Zhao, 2004). This structure is characterized by a pronounced asymmetry (Zhao, 2004; King, 2001) in relative plate movements. This asymmetry is the essence of subduction, whereby one plate moves beneath the other (Figs. 1A and 1B). Subduction processes are often studied numerically with the use of models that have this asymmetry prescribed kinematically (e.g., King, 2001; van Keken et al., 2002). However, in global mantle convection models, where this asymmetry is not prescribed, subduction is symmetrical, or "two-sided" (Figs. 1C and 1D), where downwelling involves materials from both plates (Tackley, 2000).

Recent dynamic models of subduction process, operating with realistic viscoelastic-plastic rheology (Hassani et al., 1997; Hall et al., 2003; Sobolev and Babeyko, 2005; Tagawa et al., 2007; Gorczyk et al., 2007), have shown that stable one-sided subduction requires a low strength interface between strong plates. These studies indicate that the effective friction coefficient at the subduction interface must be below 0.1 to enable stable subduction. Because such friction coefficients are lower than experimental values for dry solid rocks, the low strength interface has been attributed to the presence of metamorphic fluids (e.g., Hall et al., 2003).

Here, we explore how water influences the stability, intensity, and mode of subduction after the spontaneous initiation of a subduction zone. For this purpose, we employed a high-resolution two-dimensional viscoelastic-plastic model that accounts for metamorphic devolatilization, partial melting, and water transport.

NUMERICAL MODEL

The model (Fig. 2A) simulates subduction that is spontaneously initiated at a boundary between two oceanic plates with different ages juxtaposed along a weak transform fault (Hall et al., 2003) characterized by low plastic strength. A rectangular grid using 511×113 finite-difference points with a nonuniform spacing of 1–30 km provides resolution of 2×1 to 2×2 km in the 600-km-wide trench area of the model. Lithological structure and water propagation are resolved with 3–5 million markers.

The initial thermal structures of the two plates correspond to their imposed ages. The geothermal gradient in the asthenospheric mantle below the lithosphere is 0.5 K/km. The thermal boundary conditions are constant temperature (273 K) at the upper boundary, thermally insulated vertical boundaries, and a heat advection condition (Gorczyk et al., 2007) across the bottom of the model. The velocity boundary conditions are free slip at all boundaries except the lower one, which is permeable in both the downward and upward directions (Gorczyk et al., 2007).

The model oceanic crust consists of a 2-km-thick basaltic layer, underlain by a 6-km-thick gabbroic section. The mantle underneath is anhydrous peridotite. The phase assemblages (including melts) and physical properties for each lithology are obtained by free-energy minimization (Connolly, 2005) as a function of composition, pressure, and temperature from thermodynamic data, as summarized by Gerya et al. (2006).
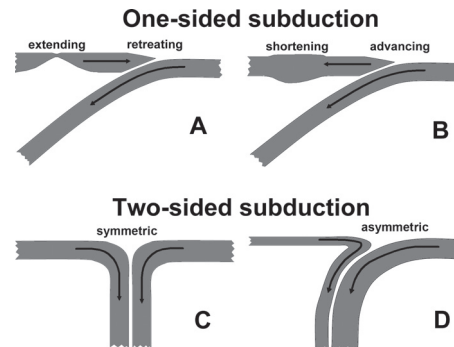
Figure 1. Various one-sided (A–B) and two-sided (C–D) subduction geometries. In case of one-sided geometries, overriding plate does not subduct. Depending on relative plate motion, overriding plate can be either extending (A) (Fig. 2C) or shortening (Sobolev and Babeyko, 2005) (B). In case of two-sided geometries, both plates subduct together. Depending on relative thicknesses (ages) of plates, two-sided subduction can be either symmetric (Tackley, 2000) (C) or asymmetric (D) (Fig. 2B).

At the onset of subduction, the oceanic crust is partially hydrated (Gerya et al., 2006), and the surrounding mantle is anhydrous. If a dehydration reaction is predicted to occur during subduction, then the released water is assumed to migrate upward until it reaches a rock that is thermodynamically undersaturated with respect to water. The velocity of water is computed from the local kinematic transport condition as

$$v_{x(\text{water})} = v_x, \quad v_{z(\text{water})} = v_z + v_{z(\text{fluid})}, \qquad (1)$$

where v_x and v_z indicate the local velocity of the mantle, and $v_{z(\text{fluid})}$ is the effective velocity of water migration through the mantle, which is assumed to be constant. Equation 1 is solved at each time step from fluid markers that contain information about the amount of transported water.

In addition to hydrous minerals, water is also present in the oceanic crust as a pore fluid (i.e., connate fluid). Pore-water content ($X_{\text{H}_2\text{O}[p]}$) is assumed to decrease linearly with depth as

$$X_{\text{H}_2\text{O}(p)} = (1 - \Delta z / \Delta z_{\text{por}}) X_{\text{H}_2\text{O}(p0)}, \qquad (2)$$

where $X_{\text{H}_2\text{O}(p0)}$ is the water content at the surface, Δz is depth below the surface, and Δz_{por} is the maximum depth for the presence of connate water.
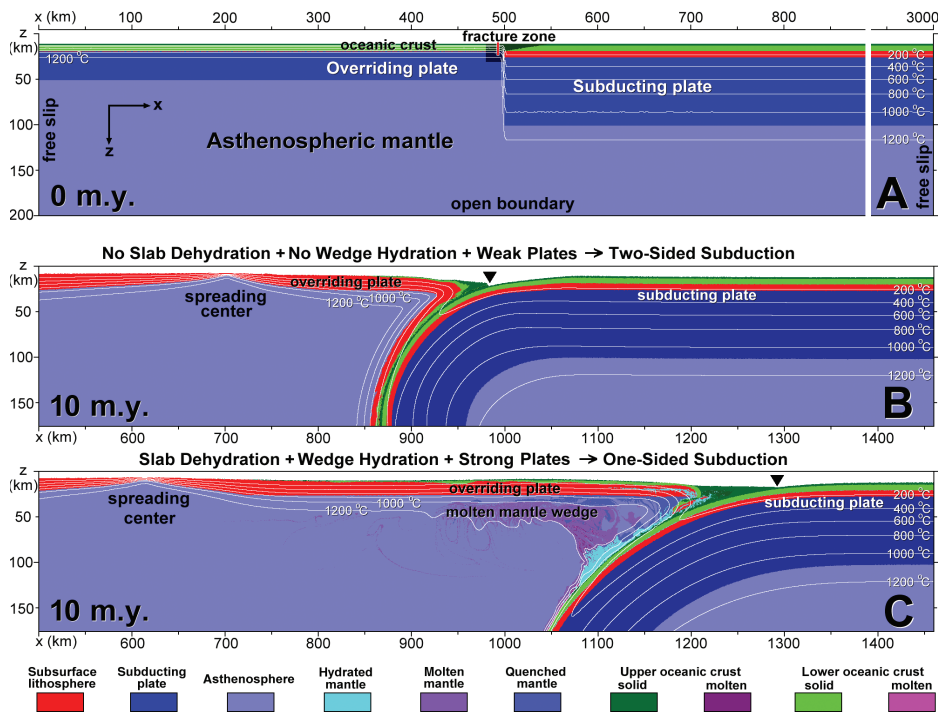
Figure 2. Two-dimensional (2-D) numerical modeling setup (A) used in this study and results (B–C) of numerical experiments showing self-sustaining two-sided (B) and one-sided (C) subduction modes. Initially (A), two plates of different ages (1 Ma and 70 Ma for the left and right plates, respectively) are juxtaposed together along a transform fault. Initial zone of wet fractured rocks with low plastic strength (sin[φ] = 0) is present along the fault (Hall et al., 2003). Subduction pattern in (B) and (C) is shown by displacement of red subsurface mantle lithosphere (i.e., dry mantle cooled below 900 °C at depths <15 km below the surface) of two plates. Stable asymmetric two-sided subduction (B) results from low plastic strength (sin[φ] = 0.1) of plates and absence of weak lubrication layer produced by slab dehydration. Stable retreating one-sided subduction (C) results from high plastic strength (sin[φ] = 0.6) of plates and presence of weak lubrication layer containing percolating fluids released by slab dehydration.

We employ a viscoelastic-plastic rheology with experimentally calibrated flow laws and elastic shear moduli computed from stable phase assemblages for each lithology (cf. Gerya et al. [2006] for rheological and petrological details). The plastic strength is taken to be dependent on pore-fluid pressure, P_{fluid}, such that (Ranalli, 1995):

$$\sigma_{yield} = C + \sin(\varphi)P, \qquad (3)$$

and

$$\sin(\varphi) = \sin(\varphi_{dry})(1 - \lambda), \qquad (4)$$

where P is pressure, C is cohesion (residual strength at $P = 0$), φ is effective internal friction angle (φ_{dry} is φ for fluid-absent conditions), and $\lambda = P_{fluid}/P$ is the pore-fluid-pressure factor. For crystalline rocks, $\sin(\varphi_{dry})$ typically varies from 0.2 to 0.9, depending on pressure, temperature, and mineralogical composition (Brace and Kohlestedt, 1980; Moore et al., 1997).

The pore-fluid-pressure factor (λ) controls the plastic strength of porous or fractured media. A hydrostatic gradient with $\lambda = 0.4$ is generally accepted for the upper crust (Sibson, 1990). As follows from studies of deep wells (e.g., Sibson, 1990) at larger depths relevant for fluid release in subduction zones (10–300 km), pressure of free porous fluid will be close to lithostatic (i.e., $\lambda \approx 1$ and $\varphi \approx 0$). Thus, the plastic strength of rocks in subduction zones is strongly dependent on the presence or absence of pore fluids. Accordingly, we assume $\sin(\varphi) = 0$ for wet crustal and mantle rocks, i.e., wherever free water fluid is present.

The governing equations of conservation of momentum, mass, and energy are solved in two-dimensions (2-D) with the use of the code I2ELVIS (Gerya and Yuen, 2007) based on finite-differences and marker-in-cell technique.

RESULTS OF SIMULATION

We carried out a total of 71 numerical experiments (see the GSA Data Repository[1]) and systematically varied model parameters, such as
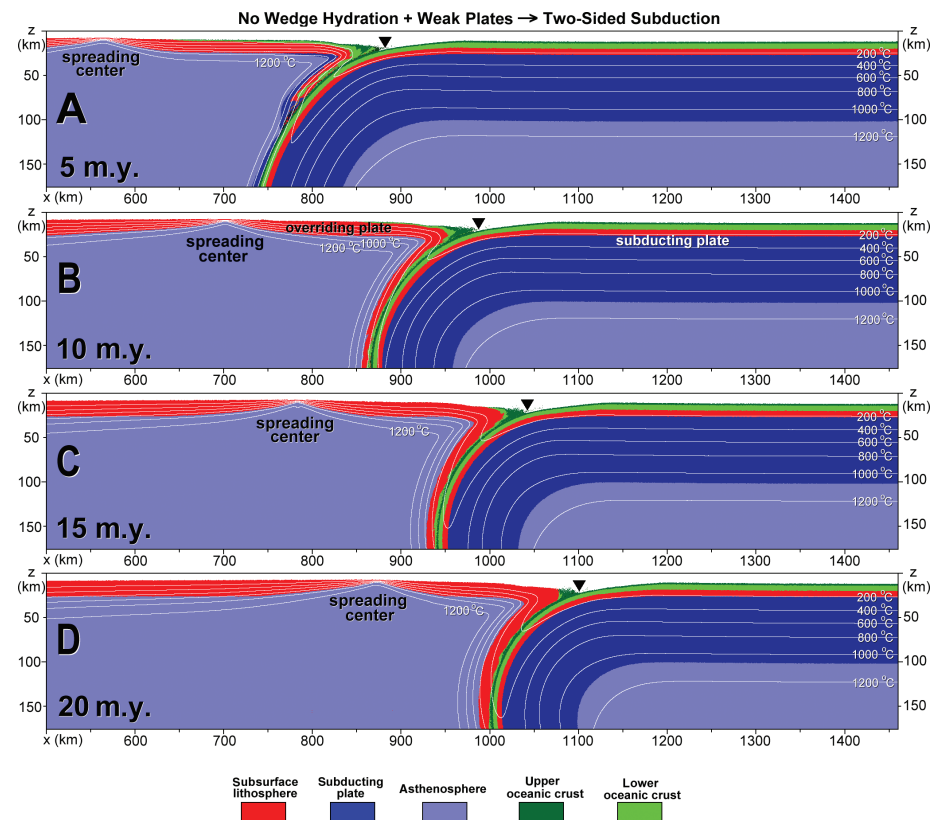
Figure 3. Results of numerical experiments (Fig. 2B) showing typical dynamics of self-sustaining two-sided subduction development. Solid triangle shows trench position.

presence or absence of water in the model, rate of fluid migration, plate ages, size of the initial weak zone, and plastic strength of crustal and mantle rocks.

Initiation of subduction depends on the size and strength of the initial weak zone. Without a weak zone, subduction only initiates if the age of the overriding plate is less then 0.5 Ma. Upon initiation of subduction, the rocks of the weak zone are sheared along the surface of the subducting plate, creating a weak layer that lubricates plate movement. The subsequent development is dependent on the plastic strength of the plates and the presence/absence of a weak hydrated layer above the descending slab. When brittle strength of the plates is high ($\sin[\varphi] > 0.15$) and no weak hydrated layer is present atop the slab, subduction ceases after several million years as a consequence of the thinning of the interplate shear zone.

Without an interplate shear zone, stable subduction is only possible if the entire slab is characterized by low plastic strength ($\sin[\varphi] < 0.15$). In this case, however, there is a strong tendency to develop two-sided subduction, in which the

subsurface lithosphere of the overriding plate is dragged downward with the subducting slab (Figs. 2B and 3).

The only scenarios in which self-sustaining retreating one-sided subduction consistently develops are those with relatively high plate strength ($\sin[\varphi] > 0.15$) and a persistent weak ($\sin[\varphi] = 0$) shear zone atop the slab. The shear zone includes both the weak upper oceanic crust, which releases the fluids, and mantle wedge rocks hydrated by passage of these fluids (Figs. 2C and 4). Hydration of mantle wedge rocks also triggers partial melting and forms a sublithospheric hydrated magmatic source region (Gerya et al., 2004; Gorczyk et al., 2007) below the overriding plate (Figs. 2C and 4).

Trench retreat occurred in all our simulations; it causes the formation of a stable back-arc spreading center, which limits the length of the overriding plate (Figs. 3 and 4). This length changes with time and increases in models with one-sided subduction (Fig. 4). In simulations with two-sided subduction (Fig. 3), the length of the overriding plate that is subducted together with the slab is reduced (cf. Figs. 2B and 2C).

DISCUSSION AND CONCLUSIONS

The domain diagram (Fig. 5) shows that the intensity of retreating subduction strongly increases with increasing volume of hydrated rocks atop the subducting slab at any slab strength. This behavior is consistent with the conclusion of Gorczyk et al. (2007), who stated that the rate of slab retreat positively correlates with the effective velocity of water transport, as this velocity controls the amount of hydrated rocks produced above the slab.

Two-sided subduction occurs at such low slab strengths ($\sin[\varphi] < 0.15$) that the presence of a weak interplate zone caused by fluid release has no significant influence on the stability of subduction. Although slab strengths of this magnitude are usually invoked to explain plate tectonics in geodynamic models (Tackley, 2000; Trompert and Hansen, 1998; Moresi and Solomatov, 1998; Solomatov, 2004), in the absence of any alternative weakening mechanism, such low strengths imply—via Equation 4—the thermodynamically implausible scenario that fluids are present throughout the slab.
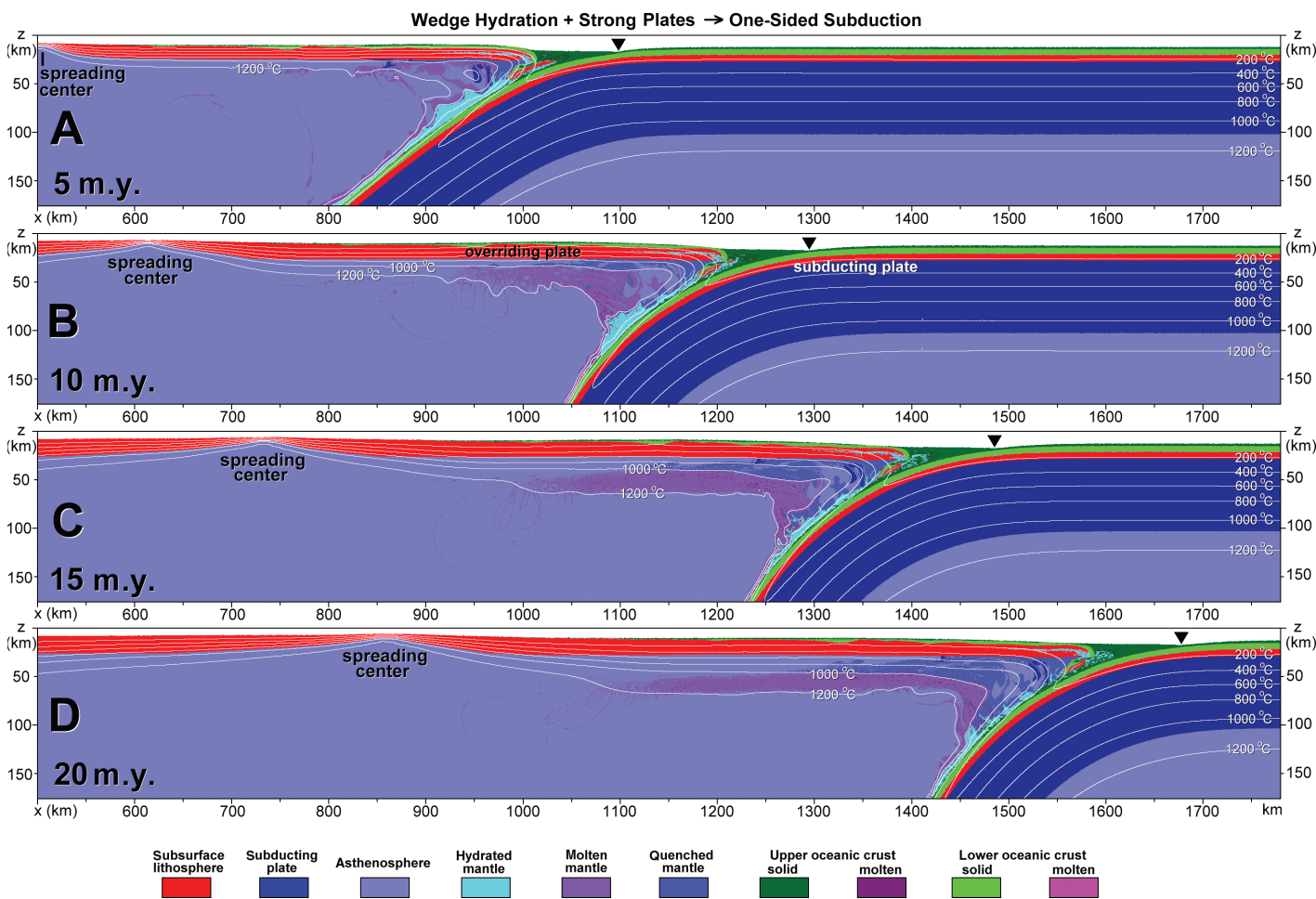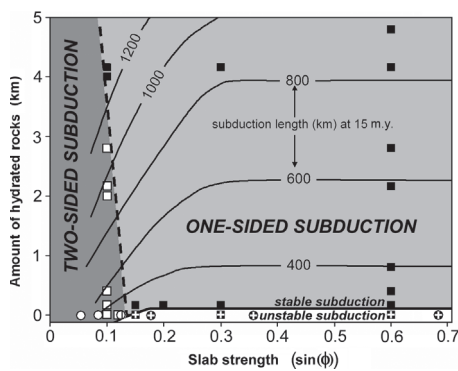

Figure 4. Results of numerical experiments (Fig. 2C) showing typical dynamics of self-sustaining one-sided subduction development. Solid triangle shows trench position.

Figure 5. Domain diagram showing stability, intensity, and mode of subduction as a function of slab strength and average amount of hydrated rocks atop the slab, i.e., bulk volume of weak (sin(φ) = 0) hydrated rocks (initial weak zone, upper crust, and hydrated mantle) normalized to entire surface of slab (km = km^3 per 1 km^2 of slab surface). Symbols correspond to conditions of numerical experiments resulting in development of one-sided (solid symbols) and two-sided (open symbols) subduction modes: squares—this study, circles—global mantle convection models investigating stability of subduction in absence of weak hydration zones (Tackley, 2000). Symbols with cross correspond to unstable subduction: subduction either does not start or ceases within fewer than 5 m.y. Thick solid line separates stable and unstable subduction fields. Thick dashed line separates one-sided and two-sided subduction fields. Thin solid lines correspond to length of subduction after 15 m.y. from beginning of experiment.

In contrast, one-sided subduction occurs at plausible (sin[φ] > 0.15) slab strengths that allow the overriding plate to sustain the bending stresses that arise from slab movement. However, one-sided subduction is only stable if weak hydrated rocks are present atop the subducting slab, i.e., subduction ceases without continuous supply of these rocks. Therefore, our models suggest that self-sustaining one-sided subduction in terrestrial plate tectonics is caused by the localization of deformation at a weak hydrated interplate shear zone, which forms as a consequence of water release from the subducted slab. This shear zone decouples the strong plates and introduces a sustainable asymmetry to plate movement. Other lines of evidence that support our contention of high strength of terrestrial plates are: (1) mantle convection models that explore weak plates are unable to explain the absence of correlation between plate age and subduction (Labrosse and Jaupart, 2007); and (2) the observed plate age distribution requires that the buoyancy of slabs is transmitted to plates by a combination of viscous drag in

the mantle and strong lithosphere (Conrad and Lithgow-Bertelloni, 2002).

Our work indicates that high plate strength and the presence of water are major factors controlling styles of plate tectonics driven by self-sustaining one-sided subduction processes on Earth. This type of subduction does not require low strength of the entire lithosphere, as has often been proposed in the past (Tackley, 2000; Trompert and Hansen, 1998; Moresi and Solomatov, 1998; Solomatov, 2004), but instead requires weakening of only the contact region between the two plates as a result of dehydration and migration of water.

REFERENCES CITED

Brace, W.F., and Kohlestedt, D.L., 1980, Limits on lithospheric stress imposed by laboratory experiments: Journal of Geophysical Research, v. 85, p. 6248–6252.

Connolly, J.A.D., 2005, Computation of phase equilibria by linear programming: A tool for geodynamic modeling and an application to subduction zone decarbonation: Earth and Planetary Science Letters, v. 236, p. 524–541, doi: 10.1016/j.epsl.2005.04.033.

Conrad, C.P., and Lithgow-Bertelloni, C., 2002, How mantle slabs drive plate tectonics: Science, v. 298, p. 207–209, doi: 10.1126/science.1074161.

Gerya, T.V., and Yuen, D.A., 2007, Robust characteristics method for modeling multiphase visco-elasto-plastic thermo-mechanical problems: Physics of the Earth and Planetary Interiors, v. 163, p. 83–105, doi: 10.1016/j.pepi.2007.04.015.

Gerya, T.V., Yuen, D.A., and Sevre, E.O.D., 2004, Dynamical causes for incipient magma chambers above slabs: Geology, v. 32, p. 89–92, doi: 10.1130/G20018.1.

Gerya, T.V., Connolly, J.A.D., Yuen, D.A., Gorczyk, W., and Capel, A.M., 2006, Seismic implications of mantle wedge plumes: Physics of the Earth and Planetary Interiors, v. 156, p. 59–74, doi: 10.1016/j.pepi.2006.02.005.

Gorczyk, W., Willner, A.P., Gerya, T.V., Connolly, J.A.D., and Burg, J.-P., 2007, Physical controls of magmatic productivity at Pacific-type convergent margins: Numerical modeling: Physics of the Earth and Planetary Interiors, v. 163, p. 209–232, doi: 10.1016/j.pepi.2007.05.010.

Hall, C.E., Gurnis, M., Sdrolias, M., Lavier, L.L., and Muller, R.D., 2003, Catastrophic initiation of subduction following forced convergence across fractures zones: Earth and Planetary Science Letters, v. 212, p. 15–30, doi: 10.1016/S0012–821X(03)00242–5.

Hassani, R., Jongmans, D., and Chery, J., 1997, Study of plate deformation and stress in subduction processes using two-dimensional numerical models: Journal of Geophysical Research, v. 102, p. 17,951–17,965.

King, S.D., 2001, Subduction zones: Observations and geodynamic models: Physics of the Earth and Planetary Interiors, v. 127, p. 9–24, doi: 10.1016/S0031–9201(01)00218–7.

Labrosse, S., and Jaupart, C., 2007, Thermal evolution of the Earth: Secular changes and fluctuations of plate characteristics: Earth and Planetary Science Letters, v. 260, p. 465–481.

Moore, D.E., Lockner, D.A., Shengli, Ma, Summers, R., and Byerlee, J.D., 1997, Strengths of serpentinized gauges at elevated temperatures: Journal of Geophysical Research, v. 102, p. 14,787–14,801, doi: 10.1029/97JB00995.

Moresi, L., and Solomatov, V., 1998, Mantle convection with a brittle lithosphere: Thoughts on the global tectonic style of the Earth and Venus: Geophysical Journal International, v. 133, p. 669–682, doi: 10.1046/j.1365–246X.1998.00521.x.

Ranalli, G., 1995, Rheology of the Earth (2nd edition): London, Chapman and Hall, 413 p.

Sibson, R.H., 1990, Faulting and fluid flow, *in* Nesbitt, B.E., ed., Fluids in Tectonically Active Regimes of the Continental Crust: Vancouver, Mineralogical Association of Canada, p. 92–132.

Sobolev, S.V., and Babeyko, A.Y., 2005, What drives orogeny in the Andes?: Geology, v. 33, p. 617–620.

Solomatov, V.S., 2004, Initiation of subduction by small-scale convection: Journal of Geophysical Research, v. 109, p. B01412, doi: 10.1029/2003JB002628.

Tackley, P.J., 2000, Self-consistent generation of tectonic plates in time-dependent, three-dimensional mantle convection simulations. Part 1: Pseudo-plastic yielding: Geochemistry, Geophysics, Geosystems, v. 1, paper no. 2000GC000036, doi: 10.1029/2000GC000036.

Tagawa, M., Nakakuki, T., Kameyama, M., and Tajima, F., 2007, The role of history-dependent rheology in plate boundary lubrication for generating one-sided subduction: Pure and Applied Geophysics, v. 164, p. 879–907.

Trompert, R., and Hansen, U., 1998, Mantle convection simulations with rheologies that generate plate-like behaviour: Nature, v. 395, p. 686–689, doi: 10.1038/27185.

van Keken, P.E., Kiefer, B., and Peacock, S.M., 2002, High-resolution models of subduction zones: Implications for mineral dehydration reactions and the transport of water into the deep mantle: Geochemistry, Geophysics, Geosystems, v. 3, p. 1056, doi: 10.1029/2001GC000256.

Zhao, D., 2004, Global tomographic images of mantle plumes and subducting slabs: Insight into deep Earth dynamics: Physics of the Earth and Planetary Interiors, v. 146, p. 3–34, doi: 10.1016/j.pepi.2003.07.032.